Journal of Structural Geology, Vol. 1, No. 3, 1979, pp. 207 to 219.

0191-8141/79/0901-0207 $02.00/0

On the production of two inclined cleavages during a single folding event; Stirling Range, S.W. Australia

C. A. BOULTER

Department of Geology, University of Western Australia, Australia

(*Received* 17 *May* 1979; *accepted in revised form* 19 *September* 1979)

Abstract—In any one area of the Stirling Range Proterozoic low-grade fold-foreland, the first phase of folding to be associated with cleavage development has generated two inclined tectonic fabrics each of which is closely related in geometry to the folds. The most likely fold history has been determined by comparing predictions of theoretical fold mechanisms against the observed field relations and strain states seen in an arenite and minor mudrock multilayer. In an initial phase of folding dominated by layer-parallel shortening, a well-spaced mica-band cleavage was, initiated, intensified, and able to maintain a near axial plane relationship, until body rotation of limbs took over at a fold dihedral angle of about 140°. The resultant 70° angle between solution cleavage and bedding on the fold limbs was preserved by flexural slip until the fold had tightened to about 100° when, for mechanical reasons, flattening rapidly became important. During this phase, a mica-film cleavage, with grain-scale spacing, developed approximately axial planar and the solution cleavage/bedding angle on the limbs was reduced to 55°.

INTRODUCTION

THIS PAPER deals with fold/cleavage relations in a fold-foreland of low metamorphic grade. In any one portion of this terrain, the first phase of folding to be associated with cleavage development has given rise to compound fabrics. It will be demonstrated that two non-parallel cleavages have been generated during single folding episodes. Also, the intersection lineations, produced by the two cleavages on bedding, are inclined to one another and are rarely parallel to either small scale fold hinges or statistically defined fold axes. The latter departures are, however, normally less than 15°.

The terrain described is a sequence of Proterozoic metasedimentary rocks found within the Stirling Range National Park, south-west Western Australia. About one kilometre of section is exposed and the assemblage of sedimentary structures is compatible with a shallow-marine shelf environment (Clarke *et al.* 1954, and Sofoulis 1958). Original mudrock is now slate or phyllite and there is a regional variation from slate in the west to phyllite in the east. Turek & Stephenson (1966) have dated the metamorphic event at 1150 Ma using whole rock Rb/Sr methods on phyllite specimens.

The literature contains several examples of fold/cleavage relations that are geometrically similar to the Stirling Range situation though varying interpretations have been presented. Harris *et al.* (1976) have described a D_1 event which induced two inclined but broadly coeval cleavages "one analogous to slaty cleavage and the other a tectonic striping produced by pressure solution". The slaty type cleavage is approximately axial planar whilst the tectonic striping is fanned about the folds. Unfortunately, in this example the cleavage/bedding intersection lineation orientation data were not presented and hence the three dimensional relations of folds and the two cleavages cannot be determined.

A number of authors (e.g. Nickelsen 1973, Geiser 1974, Ross & Barnes 1975, Beach 1977) have suggested that cleavages have developed prior to folding at about 90° to bedding. Apart from the 'slaty type' cleavage of Ross & Barnes, the early fabrics have all been tectonic striping in nature. The above studies have invoked a variety of modifications during later folding. Unfortunately an assessment of processes is often difficult as a result of incomplete description of the observed final state. Beach (1977) presents detailed information to suggest that flexural slip was the dominant folding mechanism in the examples he studied though other adjustments did occur. Geiser (1974) noted that in his material the solution cleavage is no longer perpendicular to bedding and made use of the cleavage/bedding angles as a strain measure. No mention is made of fabrics produced during folding even through the strain in this event has modified the original orthogonal bedding/cleavage angle by as much as 30°. Nickelsen (1973), however, described an early 'solution loss' cleavage followed by 'flowage' which produced homogeneous distortion of originally spherical reduction spots. The early cleavage was considered to have been formed at right angles to bedding prior to folding and the orthogonal relationship has been preserved where bedding is at high angles to the axial surface. Where limbs are nearly parallel to the axial surface the dihedral angle is about 70°, indicating deformation other than body rotation if the initial angle was 90°. In this example, the intersection lineations of the early-cleavage and bedding are often 10° away from fold hinges. From Nickelsen's description it is difficult to determine the relationship of the 'flowage' fabric to the folds, except at the closure, and also the general geometrical relation of the early solution cleavage and the flowage fabric.

Ross & Barnes (1975) have described a geometrically similar situation to that of Nickelsen's but with two early deformation events producing 'slaty type' cleavages.

The later of the cleavages is axial planar to the first phase of folding whilst the earlier cleavage is symmetrically disposed about and between 10° to 35° away from the axial plane. The authors considered it likely that the bedding/early-cleavage angle was about 90° prior to folding. The study did include strain measurements and it was, perhaps, possible to test this hypothesis with simple modelling but this was not done. Data presented showed that cleavage/bedding intersection lineations paralleled the fold axis as defined on a π plot of bedding poles. Again it is unfortunate that essential information is missing. The intersection lineations for the two early cleavages are not distinguished and it is not known if the lineations presented (Ross & Barnes 1975, fig. 13) are from both categories.

REGIONAL STRUCTURAL GEOLOGY

The Stirling Range metasediments outcrop over a roughly rectangular 70 × 15 km area whose length is oriented east–west. Two structural domains have been defined on the orientation of the folds that produce the first axial plane cleavage seen in sandstone beds. In the eastern domain these folds and related cleavage trend nearly north–south whilst in the western domain these features trend nearly east–west. In the former region the fold-related cleavage dips to the east and the folds are markedly asymmetric showing a sense of over-riding from the east, i.e. in a west–east vertical section viewed looking north the folds show sinistral vergence. Within the western zone the fold-related sandstone cleavage dips south and the folds again are markedly asymmetric with over-riding from the south. No overprinting relations have been seen between these two cleavage sets and nowhere can one set be seen to be rotated into the other. It is believed that two deformation events are involved and that the later of the two mainly developed in zones where the earliest fabrics were weak or absent (cf. Baillie & Williams 1975).

Regionally the sedimentary layers are gently dipping and right-way-up with local departures in the steep to overturned common limbs of asymmetric fold couples (adjacent antiforms and synforms sharing a short common limb). The largest fold couples (those with 50m long common limbs) often have long limb to short limb length ratios in excess of 5 to 1. Long limbs attain dips of around 40° on the southern limb of a post-main-cleavage fold which has a 135° dihedral angle and a wavelength in excess of 5 km. This superimposed fold also disorients cleavage-fold hinge lines and has a weak generated crenulation cleavage developed in some thin slate beds. Figure 1 (a) illustrates the typical geometry of the eastern domain first-cleavage folds, particularly the concentration of readings representing the gently dipping long limb (because the short common limb was worked on in some detail those readings are probably over emphasised). Figure 1 (b) shows the situation where long limbs of asymmetric cleavage-related folds have dips of 40° on the southern limb of the large gentle superimposed fold. Minor folds related to this later event may be used as an axis of rotation of the poles to bedding for the two areas, such that the bedding poles of Fig. 1(b) may be restored to the nearly horizontal situation of Fig. 1(a). In other parts of the eastern domain where long limbs are inclined by more than 10°, the fold hinge lines may be up to 27° off the 195/015 trend seen on Mount Trio (Fig. 1 a). By rotating the long limbs about the rotation axis of Fig. 1(b) as close to horizontal as possible, the hinge lines come to lie closer to the 195 bearing.

The detailed description of fold/cleavage relations will concentrate on two areas: Mondurup Peak in the

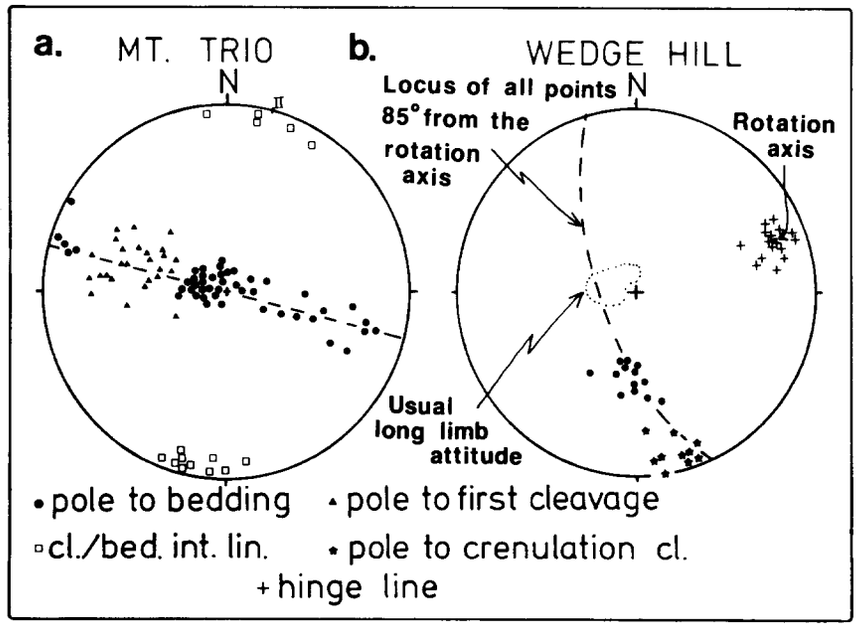

Fig. 1. (a) Geometry of Mt. Trio—an area where the long limbs of asymmetric folds are gently dipping. (b) Geometry of Wedge Hill with moderately dipping long limbs. Hinge lines of folds, with axial plane crenulation cleavage, can be used as a rotation axis to return the cluster of bedding poles to the usual gentle dip. Both are equal-area lower-hemisphere stereographic projections referred to true north.

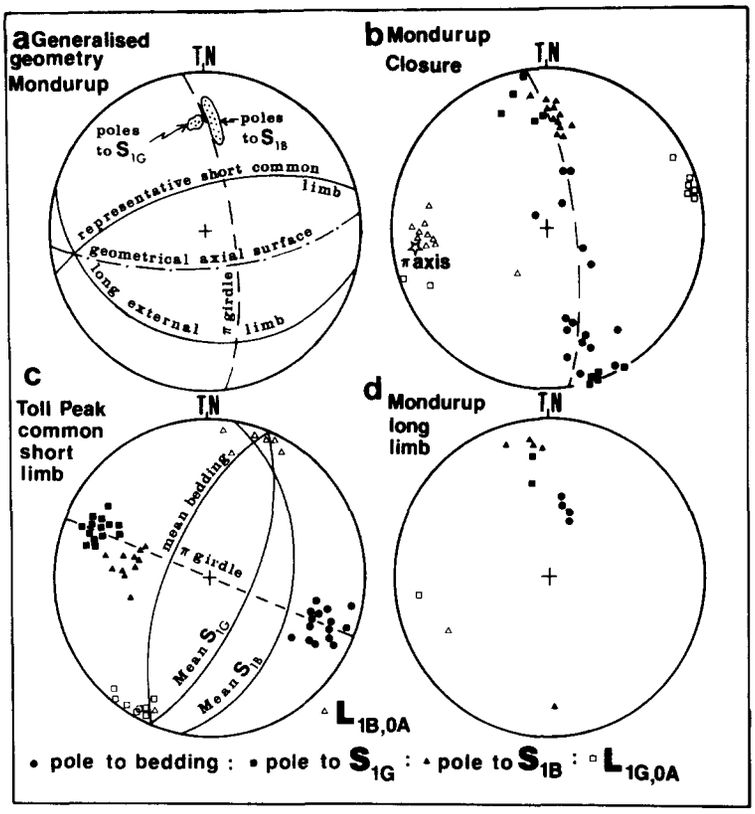

Fig. 2. Equal-area lower-hemisphere stereographic projections of structural data showing relations of bedding (S_0), the two early cleavages in the arenite (S_{1B}, S_{1G}), and the two intersection lineations ($L_{1G.0A}$ and $L_{1B.0A}$).

western domain and Toll Peak 28 km to the ENE in the eastern domain. In each locality the first phase of folding which generates a cleavage will be examined. Statistically defined fold axes on the two peaks differ in bearing by 60° (Fig. 2), a difference that cannot be explained by post-folding bulk rotation. Two phases of folding have been invoked because of the marked change between the two areas in the direction of over-riding during folding. Long limb to short limb ratios for Mondurup Peak and Toll Peak are 4 to 1 and 2 to 1 respectively. The sedimentary succession at Mondurup Peak is 95% arenite and 5% slate, whilst in contrast Toll Peak is 80% lithic wacke and 20% slate:

STRUCTURAL ELEMENTS

Quartz veins

Quartz veins both pre- and post-date the main cleavage forming episodes and show varying geometrical relations to bedding and cleavage. Bedding – parallel fibrous quartz veins are the only category of veining to be considered in detail. This type of vein may be up to 1 cm thick (Fig. 3a) and is normally entirely composed of quartz fibres lying sub-parallel to bedding. The fibre long axes are oriented sub-perpendicular to the local fold hinge lines in both areas. Of critical importance is that continuous sheets of these veins cover folds at Toll Peak without a break at the fold closure.

Other quartz vein types present include *en echelon* veins in both arenite and slate layers. Several areas are heavily intruded by pre-tectonic clastic dykes which show a polygonal or flattened polygonal intersection on bedding (cf. Nickelsen 1973). The dykes have been pulled apart and the neck zones are filled by fibrous quartz.

Mica-band cleavage

Mica-band cleavage (S_{1B}) in weathered outcrop has the appearance of 0.5 cm to 4 cm spaced joints. In fresh outcrop or thin section (Fig. 3b) this cleavage usually consists of 0.3 mm wide concentrations of mica; opaques tourmaline and zircon grains are also present and quartz is almost completely absent. The mica-bands usually cut beds completely and best, but not entirely, fit Gray's (1978) discrete rough cleavage category. The boundary between mica-bands and the host rock is sharp, and half-moon scalloped quartz grains present their straightest edge towards the band (Fig. 3b). When terminations are seen the bands pass laterally from pure mica to anastomosing networks of films where quartz progressively becomes more important and mica-films thin. Pressure solution of quartz was probably the dominant mechanism involved in the production of S_{1B} giving rise to essentially a passive enrichment of micas. In the lithons between mica-bands the fabric varies depending upon lithology. Wackes show no trace of any fabric parallel to the S_{1B} direction in the lithons and are completely dominated by an inclined fabric (S_{1G}). Arenites, however, display a weak mica-film fabric (e.g. Means 1975) in the lithons parallel to S_{1B} which is often hard to recognise because of the presence of another inclined mica-film cleavage (Figs. 3c & d). The two generations

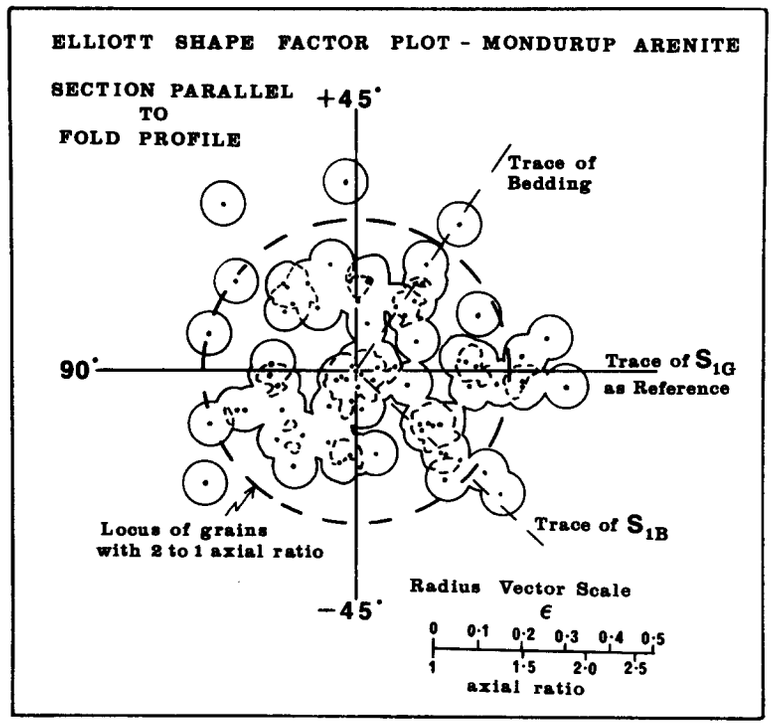

Fig. 4. An Elliott shape factor plot of 75 quartz grains from the specimen illustrated in Fig. 3(d). The one contour is a continuous line and the two contour is a dashed line. Weak preferred orientations follow the trace of S_{1G} and S_{1B}.

of mica-films are shown in Fig. 3(d) and the marked directions correspond to the fabrics seen in the field and also to maxima of grain orientations as determined on an Elliott shape factor plot of the same thin section (Fig. 4).

Mica-band width varies and, where this cleavage type has a spacing greater than 5 cm, the bands are thin (<0.2 mm) and become more difficult to identify in the field. Spacing is usually much reduced in a fold closures in comparison to adjacent limbs and locally in closure the cleavage approaches the 'very strong' type of Alvarez *et al.* (1978). Estimates of solution shortening (Plessman 1964) are difficult to make because of small irregularities in bedding surfaces caused by ripples, load casts, and the like. The intersection of mica-bands and bedding is normally associated with a sharp step in the bedding surface; the height of the step being related to the width of the mica-band. With well-developed band cleavage, the intersection lineation on arenite surfaces ($L_{1,0A}$) is regular, usually being accentuated by the etching out of mica from the cleavage to form a groove on bedding.

Grain cleavage

Grain cleavage (S_{1G}) in the field, in arenites and wackes, appears to be a dimensional preferred orientation of detrital grains. Microscopic examination of arenites, however, shows that, where almost every grain has an axial ratio of less than 2 to 1, and where preferred orientations are weak, the field expression is mainly weathering of mica films; dimensional preferred orientation of detrital grains or of muddy matrix could not be the main fabric producing elements in such material. The microscopic expression of the grain-cleavage is largely dependent upon lithology. In wackes, mica films are continuous, quartz grains are inequant parallelling the cleavage, and mica flakes show a strong preferred orientation parallel to the mica films (homogeneous type of Means 1975). All these elements define the S_{1G} direction with little fluctuation in orientation. Arenite fabrics are not as straightforward and though mica films are still the predominant fabric element, they are transitional between Gray's (1978) continuous and discontinuous types (Fig. 3d). Quartz grains are inequant, but have only low axial ratios, and show only weak alignment in cleavage. A shape factor plot of an arenite (Fig. 4) shows a tendency for quartz grains to have a slightly greater degree of preferred orientation in S_{1B} and S_{1G} than in any other direction. Pressure solution processes are again considered the best explanation for the mica films and also the related preferred orientation of quartz grains as seen in the wackes.

Between two adjacent quartz grains, mica platelets (mica-beards) have a constant strong preferred orientation, but from place to place within a thin section, this direction varies: it may either parallel S_{1G} or S_{1B} (Fig. 3c) or more rarely lie somewhere between. The perfect alignment of mica platelets between quartz grains is found in specimens such as that illustrated in Figs. 3(d) and 4, where the specimen scale strain must be very low. Also in these samples the internal strain within quartz grains must also be slight, as evidence by the low degree of undulosity (quartz *c*-axis mismatch in single grains is only a few degrees). Mica platelet orientation could not have formed by rotation of earlier micas; recrystallisation of a muddy matrix under the influence of a stress difference is favoured. Their origin as fills of dilating cracks (Means 1975) appears to be an unlikely general

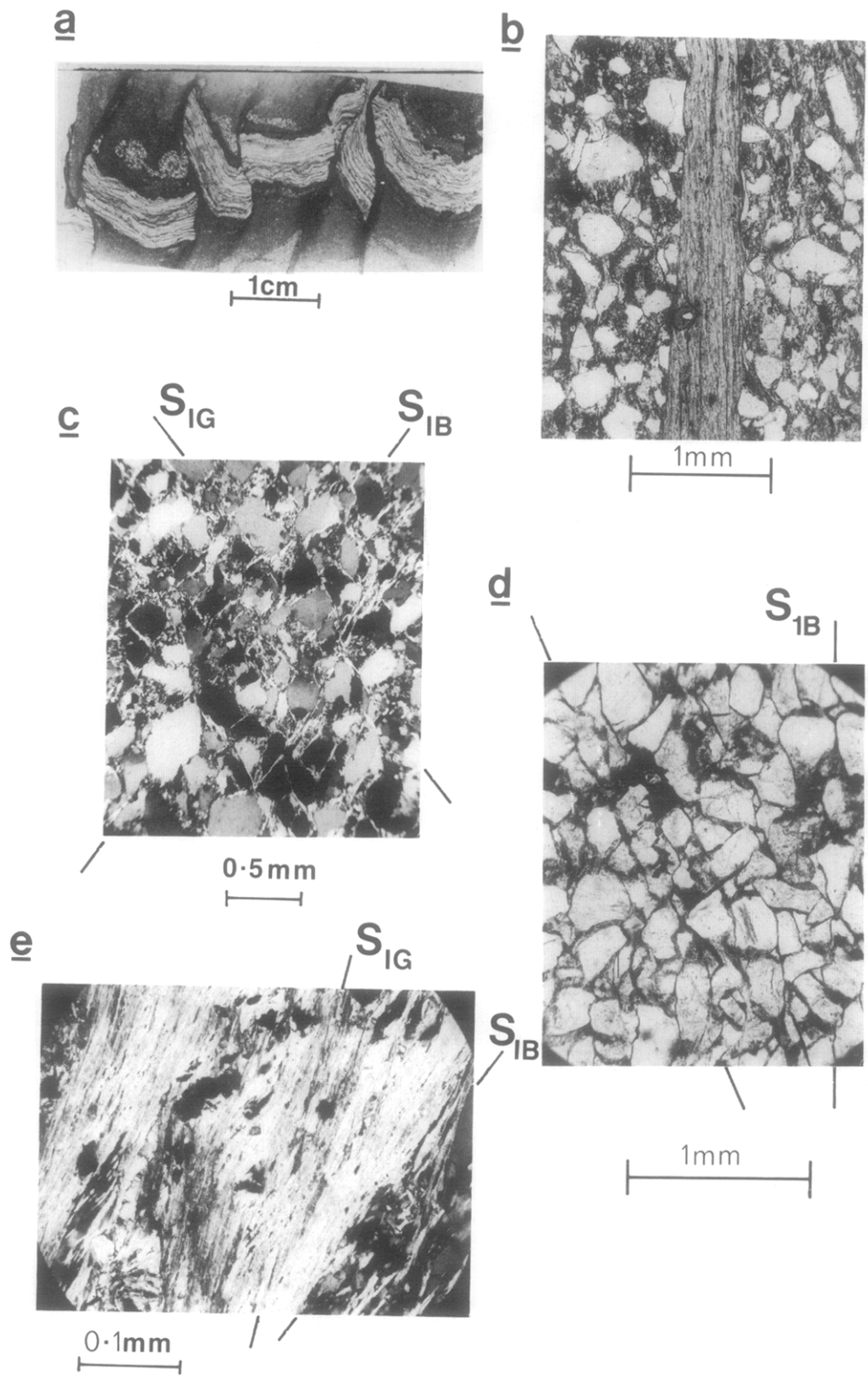

Fig. 3. (a)Bedding parallel fibrous quartz vein subdivided by mica-bands (dark). (b) Mica-band cleavage in wacke with mica-beards (S_{1G}) in the intervening material inclined to the length of the band. (c) Detail of an area between S_{1B} planes showing micas parallel only to S_{1B} and S_{1G}. (d) Arenite from Mondurup Peak cut parallel to the fold profile plane. Mica films and elongate grains define both the mica-band and grain cleavage direction. (e) Micas within a mica-band showing open crenulations whose axial surfaces are at a low angle to S_{1B}.

mechanism as muddy matrix would be present in the rock between detrital quartz grains. Very rare 'pull-aparts' have been noted with oriented micas between, but generally the quartz grain shapes do not support this mechanism.

The intersection lineation resulting from the interaction of the grain cleavage and bedding ($L_{1G,0A}$) may be difficult to observe in arenite but is generally quite clear in wacke.

Slaty cleavage

Slaty cleavage (S_{1S}) is readily seen to be a domainal fabric when viewed in thin section under plane polarised light. The main fabric element is a series of sub-parallel fine dark lines spaced between 0.01 and 0.02 mm. The lines are largely defined by concentrations of opaques though in crossed polars they are also seen to be bands of aligned fine micas. Stubby chlorites are found between adjacent dark lines (cleavage planes), either as equant grains or with slight elongation parallel to the cleavage. The chlorite 001 planes are close to the bedding direction and usually at a moderate or high angle to the rock cleavage. Following the work of many authors (e.g. Beutner 1978) the chlorites are probably remnants of larger detrital chlorites that have been corroded by solution transfer during deformation. Clear micas, other than those in the cleavage bands, have a variety of orientations and commonly have aspect ratios greater than 4 to 1 where the 001 planes parallel the grain length. Several of these micas cut three or more rock-cleavage planes at high angles, and deflect the planes at their margins. Such features suggest that the clear micas, while perhaps undergoing some solution transfer during deformation, are more resistant to chemical modification than the chlorites, and deform to a greater degree by body rotation. The relative importance of these processes is impossible to evaluate on the basis of transmitted light investigations.

FOLD/CLEAVAGE GEOMETRY

The geometrical relations will be initially illustrated using the most regular case of sub-angular folds where all information is obtained on the limbs (Fig. 5a). Rather than following the normal convention of down plunge viewing, the viewing direction of the fold profiles has been standardised such that they all have '*Z*' asymmetry. Plunges are all gentle and any variation is usually attributable to a later deformation. Having a standard view allows a more straightforward comparison of cleavage/bedding relations from fold to fold particularly from the short limb of one fold to the long limb of another.

The fold seen in Fig. 5(a) is sub-angular, has an 80° dihedral angle, and has a 30° dip to the long external limb. The latter value has been increased by subsequent rotation of the whole fold and long limb dips are nor-

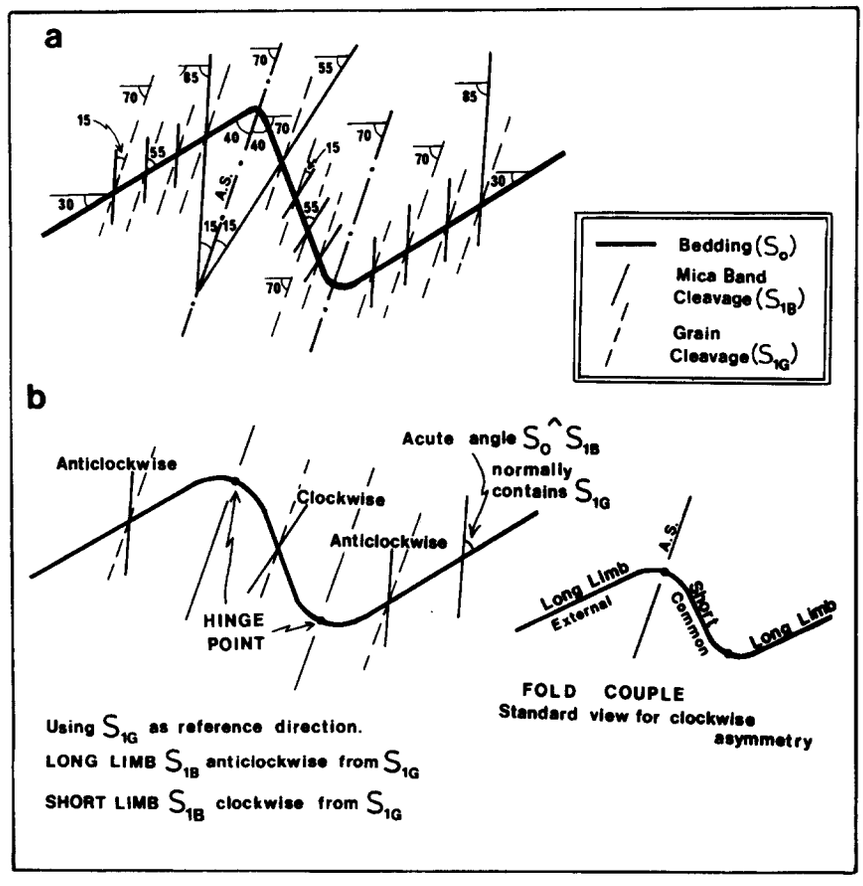

Fig. 5. (a) Profile view of the sub-angular fold at the NW end of Mondurup ridge. The outline is generalized. (b) Nomenclature used in describing the asymmetric folds and geometric relations of the grain and mica-band cleavages.

mally between 5 and 10°. The illustrated fold is from Mondurup and structural readings have been averaged, though in the sub-angular examples attitude variation is limited.

The grain cleavage (S_{1G}) is nearly constant in orientation throughout both limbs, and has nearly an axial planar relationship to the fold. On both long and short limbs, the bedding/grain cleavage angle is close to 40°. The mica-band cleavage (S_{1B}) displays a near symmetric convergent fan of 15° on either side of the axial surface, and on both limbs the S_{1B}/bedding angle is approximately 55°. Stereographically, these relations result in a spread of poles to S_{1B}, and a centre concentration of poles to S_{1G}, as seen in a generalized view (Fig. 2a). In the sub-angular fold, the acute angle between bedding and S_{1B}, always contains the grain cleavage (Figs. 5a & b). Using S_{1G} as the reference, it therefore follows that on the long limb S_{1B} is anticlockwise S_{1G} (Figs. 5a & b).

Several sub-rounded closures have been examined in detail (Figs. 6 and 7) and these have revealed a more complex geometry than the limbs. Because the folds are reconstructed from discontinuous outcrop, the hinge point on a single surface could not be located by inspection. On the diagrams its position can only be given in very general terms. Hence, a hinge surface cannot be constructed and the figures show the orientation of the bisector of the interlimb angle to act as a reference when comparing angular (Fig. 5) and more rounded folds (Figs. 6 and 7). On profile planes, where bedding traces are perpendicular to the fold bisector trace, this point should be close to the hinge point where layer thicknesses show a symmetric variation on both limbs; this approach is used here to give the approximate location of the hinge point.

The fold represented in Fig. 6 (see also Fig. 2b) maintains, for the most part, the relationship of S_{1G} being in the bedding/S_{1B} acute angle with the exception of the region close to the hinge point (station 5). Here S_{1G} is in the bedding/S_{1B} obtuse angle. Another variation is that, in the closure, towards the common limb side of the approximately located hinge point, the S_{1G} cleavage fans away from the axial surface (Fig. 6, stations 7 to 13). When the limb becomes straight (stations 14/15), the regular short limb relation of the sub-angular fold (Fig. 5a) is achieved.

Figure 7(a) gives the cleavage relations in the closure of a sub-rounded fold where stations 2 to 5 show S_{1G} in the S_0/S_{1B} acute angle and station 1 is anomalous. Even though stations 1 and 2 are close to the long limb of the fold they both have S_{1B} clockwise from S_{1G}; the usual short limb relation. Further complexities are found in large dihedral angle folds (Fig. 7). On the short limbs, S_{1B} shows the more typical clockwise relation to S_{1G} but in Fig. 7(b) (i) and (ii), S_{1G} is in the S_{1B}/S_0 obtuse angle. A similar obtuse relation holds on the long limb of Fig. 7(b) (iii) and also the clockwise S_{1B} from S_{1G} relation is in contrast to most long limb observations. Such complexities appear to reflect complex strain histories in the closures. Beyond a distance equivalent to the length of the short limb, the cleavage relations on the long limbs become less clear. In such areas, S_{1B} and S_{1G} become very close in dip and strike, and it is difficult to be certain whether S_{1G} always falls in the bedding S_{1B} acute angle. Both fabrics decrease in intensity away from the long limbs and, at some distance from the closures, the mica-band cleavage is not perpendicular to bedding.

The geometry of the fold shown in Fig. 6 is plotted in Fig. 2(b). Sixteen poles to bedding were used to define the dashed π girdle line and the π axis. Both poles to S_{1G} and S_{1B} tend to fall off this girdle, particularly the cluster of near vertical S_{1G} reading from the closure on the short limb side of the hinge point (stations 7 to 13, Fig. 6). Neither intersection lineation, $L_{1G,0A}$ or $L1_{B,0A}$ are

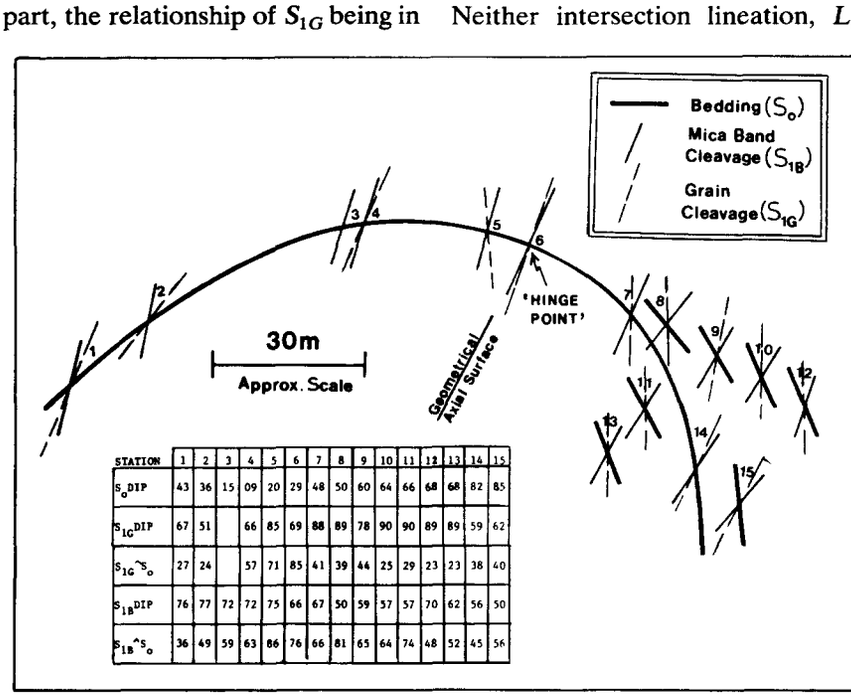

STATION	1	2	3	4	5	6	7	8	9	10	11	12	13	14	15
S_o DIP	43	36	15	09	20	29	48	50	60	64	66	68	68	82	85
S_{1G} DIP	67	51		66	85	69	88	89	78	90	90	89	89	59	62
$S_{1G} \wedge S_o$	27	24		57	71	85	41	39	44	25	29	23	23	38	40
S_{1B} DIP	76	77	72	72	75	66	67	50	59	57	57	70	62	56	50
$S_{1B} \wedge S_o$	36	49	59	63	86	76	66	81	65	64	74	48	52	45	56

Fig. 6. Profile view of a sub-rounded fold, Mondurup Peak. Reconstructed from scattered outcrop and, hence, the bedding trace, hinge point, and geometrical axial surface, are used to indicate the fold features in a general way.

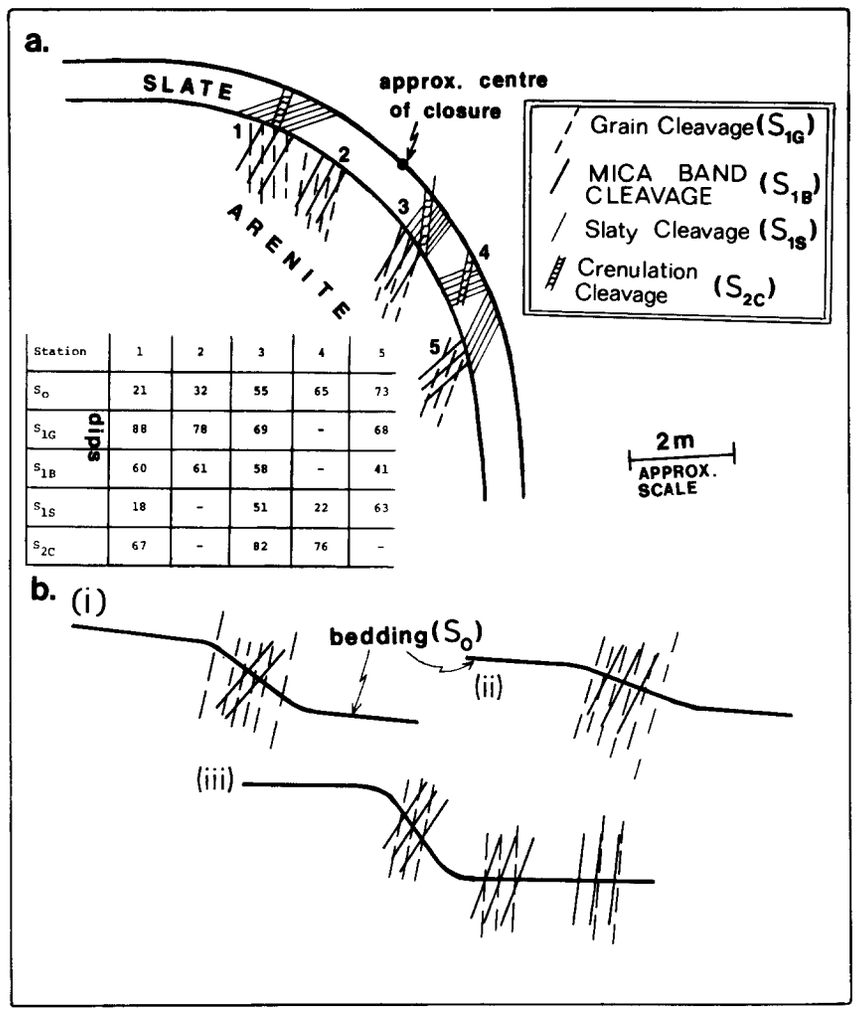

Station	1	2	3	4	5
S_0	21	32	55	65	73
S_{1G} dips	88	78	69	-	68
S_{1B}	60	61	58	-	41
S_{1S}	18	-	51	22	63
S_{2C}	67	-	82	76	-

Fig. 7. (a) Profile view of a sub-rounded fold, Toll Peak. Again relations between observation points are indicated in a general way. (b) Sub-angular, open folds from Toll Peak.

coincident with the π axis, though the latter is closest. The $L_{1G,0A}$ readings are heavily influenced by data gathered from stations 7 to 13, and are somewhat unrepresentative.

Much better definition of fold geometry can be obtained from Toll Peak where there is no differential rotation of segments due to later events. The π girdle drawn on Fig. 2(c) was based on 59 bedding readings from long and short limbs, and closures. Figure 2(c) however, concentrates on plotting data from the short limbs only and shows a clear separation of S_{1G} and S_{1B}' and that here S_{1B} poles are off the statistically defined π girdle. $L_{1G,0A}$ tends to be close to the statistical π axis, while $L_{1B,0A}$ is found on a distinctly different bearing. Meagre data from a long limb situation (Fig. 2d) show the anticlockwise S_{1B} from S_{1G} relation of Fig. 5(a).

Slaty cleavage displays an overall divergent fan. On long limbs, the slaty cleavage dip and strike is quite regular, whereas within the closures and on the short limbs some variation is found. Small open folds on the short limbs cause further fanning of the slaty cleavage. Orientation changes, such as those between stations 3, 4 and 5, in Fig. 7(a), are often related to irregularities in sedimentary units. Where slaty cleavage has a low dip (i.e. from around the hinge point out towards the long limb), a crenulation is developed with a very similar dip and strike to S_{1G} in the adjacent sandstone. This crenulation only appears in fold closures where S_{1G} fabrics are best developed.

SEQUENCE OF EVENTS

Overprinting relations show the following order of development; bedding-parallel fibrous quartz veins first, mica-band cleavage and then grain cleavage. Of critical importance is the time of fold initiation in this sequence, and this question is the main subject of the following section.

Individual fibrous quartz veins normally consist of segments in cross-section, 1 to 2 cm long and about 5 to 6 mm deep. Each segment has the form of a single open fold and adjacent portions are usually concave in the same sense (Fig. 3a). The segments are bounded by S_{1B} planes and offsets along successive planes are consistent in sense where the veins are inclined at less than 90° to S_{1B}. The majority of the segments maintain a near constant thickness between adjacent S_{1B} planes. Such features suggest segmentation of once continuous layers by

development of concentrated discrete zones of pressure solution. The internal fibres of the veins indicate relative displacement between adjacent beds which would have a component of bed separation but with a major component parallel to the layers. If S_{1B} was initiated during such displacement, i.e. during the vein growth, the mica bands would be expected to show pronounced and consistent curvature: this is not observed and S_{1B} is believed to entirely post-date this generation of fibrous quartz veins.

Pure mica layers of the S_{1B} cleavage in arenite are internally crenulated, on a small scale (Fig. 3e), in an orientation which is very close to that of S_{1G} in the microlithons. Such an overprint cannot be detected on the mica films that lie parallel to S_{1B} in the material between S_{1B} planes (Figs. 3c & d). The fineness of the crenulations in the micas suggests that such structures may not survive the grain growth associated with a slight increase in temperature and thus may account for a lack of overprint noted by Harris *et al.* (1976) in a similar situation but in slightly higher grade rocks.

S_{1G} is also usually found in the acute angle between S_0 and S_{1B}, suggesting that the latter two surfaces have converged during the strain associated with formation of S_{1G}, thus strengthening the overprinting evidence. The sense of refraction of the inclined fabric through the mica-bands is inconsistent with the bands being a crenulation fabric developed during folding. A coeval, syn-folding, origin for both S_{1G} and S_{1B} appears unlikely and also offsets of bedding along S_{1B} are consistent with simple removal of a certain width of material rather than being related to crenulation processes.

Fibrous quartz veins of the type found in the Stirlings are normally considered to be syn-folding (e.g. Beutner 1978) being caused by flexural slip. If the present veins follow the standard pattern, then it would follow that both S_{1B} and S_{1G} were syn-folding. Nicholson (1978) has, however, come out in favour of pre-folding veins of a similar fibrous bedding-parallel nature, and in the Stirlings the veins are found to completely cover folded surfaces going from one limb over a closure and on to the next limb without a break. Following Cave (1978) it seems that this relation is best explained by the fibrous quartz vein growth, and associated displacement, occurring before folding.

The timing of S_{1B} with respect to fold initiation is still uncertain as a result of the above considerations. The symmetric distribution of S_{1B} about the angular folds (Fig. 5a) suggests the fabric was either developed at right angles to bedding prior to folding or as an axial plane fabric during folding. The final state (Fig. 5a) requires that, with either of these two timings of S_{1B} growth, further modifications during folding have to take place including body rotation and strain on the scale of arenite layers. The required strain in each case can be calculated, and grain shapes within the arenite layers can be measured to estimate actual strain states. It has been argued that, in certain circumstances, grain shapes do not reflect total strain of some units because grain boundary sliding was an important deformation mechanism (e.g. Borradaile 1979). It therefore becomes critically important to consider the condition of the sediments from the time of fibrous quartz vein formation to the development of S_{1G}, the last recognisable fabric.

This discussion is centred on the Mondurup example where the multilayer contains very little mudrock ($\approx$ 5%) and hence pore fluid loss during overburden loading would not be expected to be markedly inhibited. The arenite in this area shows remnants of quartz overgrowths on detrital grains showing a degree of cementation. Approximately 80% of the binding agent in the arenite is now recrystallised and hence it is difficult to assess the amount of cement at the time of deformation. Pure quartz arenite in the succession does show complete preservation of quartz overgrowths with little remaining pore space. Bedding-parallel quartz veins are more common in the wacke/slate alterations and this may reflect entrapment of water during compaction which, during early tectonism, induces brittle behaviour (e.g. Price 1975, Beach 1977). The veins themselves mark an episode of dewatering and perhaps the development of fractures may suggest that the surrounding rock was sufficiently coherent (lithified) to support regular vein walls.

High pore fluid pressure in poorly lithified material would considerably reduce stresses at grain/grain contacts (e.g. Lisle 1977) and, under such conditions, the initiation and growth of the mica-band cleavages are difficult to envisage. Further support for a well lithified condition during fabric development comes from the detrital/diagenetic chlorites. Their 001 planes are at low angles to bedding and many have folded to produce axial planes parallel to the rock cleavage. Such features suggest the grains were not free to rotate. Also between S_{1B} planes the intervening rock usually contains fine white micas parallel to both S_{1B} and S_{1G} (Fig. 3c). If grain boundary sliding had occurred during S_{1G} development, the earlier micas might be expected to have undergone rotations with respect to one another or to the S_{1B} planes.

The above evidence is interpreted as implying a well lithified state for the arenite layers of Mondurup during S_{1B} and S_{1G} formation and that the wacke/slate alternations probably underwent a significant dewatering when the pre – S_{1B} fibrous quartz veins developed. High pore fluid pressures probably obtained during folding but it is believed that the arenite was well cemented at this time. Several horizons show massive, pre-cleavage, sandstone-dyke injection, reflecting an early dewatering event. Fabrics in these areas are similar to the general situation and further support the contention of advanced lithification prior to deformation.

FOLD HISTORIES

The majority of authors describing situations similar to the Stirlings example have come out in favour of the mica-band type cleavage pre-dating folding and having an orthogonal relationship with bedding (Nickelsen 1973, Geiser 1974, Beach 1977). Harris *et al.* (1976),

however, believe that the mica-banding developed during folding and the following argument attempts to demonstrate which pattern holds in the Stirlings; again concentrating on the Mondurup area.

For the present conditions (layered sedimentary rock, low metamorphic grade), the feasible fold mechanisms have been considered. In each case theoretical predictions of final geometry and strain state have been compared with the Mondurup example (Fig. 5a). A primary constraint on the goodness of fit between theory and field observation is the comparison of strain state. The previous section argued that the well lithified state of the arenite meant that strains would be reflected in grain shape modification. The arenite in the Mondurup fold multilayer is relatively uniform and it is believed that the fabric shown in the shape factor plot of Fig. 4 is representative of the general situation. The measured thin section was cut parallel to the profile plane and, throughout the following discussion, strain ratios are computed for each fold mechanism in this plane. Figure 4 was prepared using the method of Elliott (1970) and shows that 75% of the quartz grains have axial ratios less than 1.75 to 1. The plot is similar to specimens with slight or no strain (Boulter 1976) and demonstrate a very low strain state on the sample scale; 1.5 to 1 appears to be an upper limit.

Taking the first view ($S_{1B} \perp S_0$ pre-folding), several deformation sequences during folding are possible (i) flexural flow, (ii) flexural slip followed by or combined with fold flattening; (iii) an interaction of flexural slip, flexural flow, and flattening.

History (i) involves simple shear on arenite bedding surfaces being transmitted through the layers and the resultant distortion producing S_{1G}. If the generated tectonic fabric approximates the XY plane of the accumulated strain (Ramsay & Graham 1970), a fold with the geometry of the Mondurup example (80° dihedral angle, Fig. 5a) has a maximum elongation direction at 33° to bedding; this is within 7° of the observed S_{1G} orientation. The same distortion would reduce the initial S_{1B}/S_0 angle of 90 to 48° (angular shear strain, ψ, of 42°, Ramsay 1967) whereas the observed angle, is 55° ($\psi = 35°$). The strain ratios associated with these two angular shear strains are 2.38 to 1 and 1.99 to 1 respectively. The latter value could be achieved if flexural slip took up a component of the strain. Apart from slip on arenite/arenite contacts, arenite layers could possibly, bodily rotate while the intervening mudrock layers were deformed in simple shear.

The required strain is in excess of that measured in the Mondurup arenite material and hence this mechanism appears inapplicable in this case. The intensification of S_{1B}, and the presence of S_{1G}, in the closures implies that some mechanism other than flexural flow/slip operated. These features suggest the action of a fold-scale homogeneous strain at some stage.

The effects of mechanism (ii) can be calculated assuming bedding and S_{1B} were rotated bodily by flexural slip and then flattened symmetrically about the axial surface. In such a stepwise process the fold dihedral angle must have been about 120° prior to flattening (Fig. 8a). To take the fold from this state to the final geometry (Fig. 5a) a strain ratio of 2.1 to 1 is required. During flattening (homogeneous strain) S_{1B} and bedding converge on the axial surface (S_{1G} at Mondurup), and the fold dihedral angle is reduced to 80°. Homogeneity is on the scale of the folds, on the grain scale deformation is dominantly heterogeneous mass transfer which produces S_{1G}. The flattening process also explains the usual position of S_{1G} in the bedding/S_{1B} acute angle.

Mechanism (ii) involves strain states that are again much higher than the observed values. In an attempt to develop a mechanism which produces lower predicted strains, a combination of flexural slip, flexural flow, and flattening was considered (mechanism (iii)). By taking Fig. 8(b), one possible example of mechanism (iii) may be illustrated where flexural slip/flow is responsible for an angular shear strain of 20° on S_{1B} and homogeneous strain further reduces the S_{1B}/bedding angle to that of Fig. 5(a). The strain ratio for each component, and their sum, may be calculated and compared with other mechanisms. For a dihedral angle of 100°, ψ predicted is 35° and the modelled value of 20° (Fig. 8b) is an indication of the flexural slip component in this stage. For $\psi = 20°$ the strain ratio is 1.40 to 1 and the maximum elongation would be inclined at 10° to the axial surface. Homogeneous strain of 1.4 to 1, with an XY plane parallel to the axial surface, is required to convert Fig. 8(b) to 5(a). The resultant total strain is 1.94 to 1 with a maximum elongation 4° away from the S_{1G} direction. Other combinations of fold scale homogeneous strain and flexural slip/flow give higher total strains within arenite layers and are even more difficult to reconcile with the low strain states observed in the arenite.

The last fold history (iv) involves a sequence of events that in most of its major features is very similar to that put forward by Beutner (1978) in the summary of his paper. It has been shown that layered sequences, where viscosity contrasts exist, first respond to lateral loading by layer-parallel shortening (Hudleston 1973). The amount of strain in this phase varies with the viscosity contrast between competent and incompetent layers, but the transition to a phase of dominant limb rotation takes place when the folds have mean 'limb dips' of 10–20°, no matter what the viscosity contrast ('limb dip' is dip from the normal to the axial surface). It is proposed that in the Mondurup example, distortion during layer-parallel shortening gives rise to the mica-band fabric which develops axial planar to the folds. Because of the low ratio of fold-amplification to layer-parallel strain, the amount of body rotation of the S_{1B} cleavage as it forms is low and the fabric is capable of maintaining an axial plane, or near axial plane, relationship. Limb rotation at a dihedral angle of about 140° becomes the important process and the most reasonable strain pattern here is flexural slip or its modified version where the strain is taken up in the mudrock. This behaviour would preserve a bedding/S_{1B} angle of about 70° during body rotation of the fold limbs. Once the fold reaches a dihedral angle of about 100° (Fig. 8b), homogeneous strain

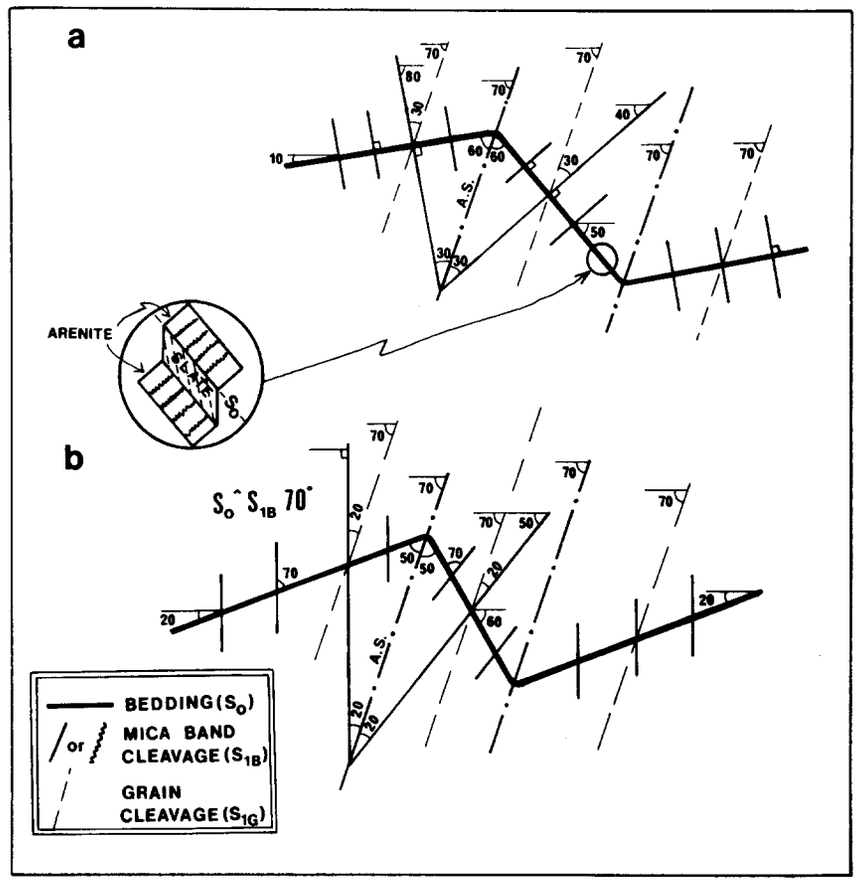

Fig. 8. (a) If S_{1B} were perpendicular to bedding prior to folding and the fold history was flexural slip followed by flattening, the fold geometry prior to flattening must have been close to that shown here. No other combination of dihedral angle and S_{1B}/axial surface angle can give the final observed geometry (Fig. 5a) with a fold scale homogeneous strain. (b) One possible combination of flexural flow/slip and flattening is shown here. If flexural flow/slip produces a 100° dihedral angle fold with an angular shear strain of 20° on the original 90° S_{1B}/S_0, then flattening can produce Fig. 5(a) with a strain ratio of 1.4 to 1. The interaction of the flattening and flexural flow components produces a resultant strain of 1.9 to 1 with a maximum elongation close to the axial surface.

of the whole fold takes over. The strain ratio to convert Fig. 8(b) to 5(a) is about 1.4 to 1 and fits the observed states extremely well.

If flexural flow is the mechanism that takes the fold from the layer-parallel shortening stage to that shown in Fig. 5(a), it can be shown that the required strain ratio is 1.69 to 1. Even though flexural flow produces a maximum elongation of almost the correct orientation (within 2° of S_{1G}) the strain is still in excess of that observed and the history of the fold must be 'flexural slip' at this stage.

If S_{1B} planes were well developed prior to folding, they could only maintain their axial surface orientation during layer-parallel shortening by growth of the bands, if significant strain in the intervening material is to be avoided. As a result the S_{1B} fabric might be expected to be intense, whereas the angular relations of Fig. 5(a) are independent of S_{1B} intensity. In contrast to Nickelsen (1973) and Geiser (1974), it is believed the S_{1B} cleavage was produced during an episode where the fold dihedral angle changed from 179° to about 140°, and not before this phase. The proposed history for the Mondurup example places limitations on the use of the S_{1B}/bedding angle as a strain gauge (cf. Geiser 1974). The angle to be modified by later distortions, in this case, is close to 70° rather than 90°, thus lessening the strain required in post-layer-parallel shortening processes. If approximately symmetric folds are produced locally within competent layers, the unfolded portions (i.e. where layers are parallel to the enveloping surface) will show S_{1B} perpendicular to S_0. It follows that an orthogonal relationship of this type cannot be taken to show pre-folding growth of S_{1B}.

CONCLUSIONS

Prior to folding, stress difference produced slip along bedding surfaces in coherent well-lithified rocks in a direction nearly at right angles to the hinges of the later developing folds. As a result of this movement, fibrous quartz veins grew sub-parallel to bedding. It is interesting to note that these features are normally taken to demonstrate the action of flexural slip during folding. Obviously such interpretations have to be treated with caution in the absence of conclusive evidence.

Several fold mechanisms and their combinations operating on two initial configurations were tested against the observed final state. The investigation considered a variety of fold histories with a range of fabric to fold timing relations. The geometry and strain state of the sub-angular Mondurup fold best fits the development of the two inclined cleavages (S_{1B} and S_{1G}) during

the folding. The intersection lineation, S_{1B} on bedding, is usually within 10° of fold axes and lineations, as would be expected if S_{1B} were syn-folding. The mica-band cleavage developed during a phase of layer-parallel shortening. Presumably, a certain amount of strain is required before the effect on the fabric is noticeable, but the S_{1B} cleavage was probably initiated when limb dips were only a few degrees. Perhaps the formation of S_{1B} is triggered by the application of stress differences at a critical time when dehydration reactions are occurring within the clay component of the sedimentary pile and releasing water in bursts (Fyfe 1976).

The main development of the S_{1B} cleavage ceased at the change from layer-parallel shortening to limb rotation, and at this point the S_{1B}/bedding angle would be about 70°. Flexural slip must have operated during limb rotation either as slip on bedding surfaces or with mudrock layers deforming under simple shear, thus leaving the S_{1B} bedding angle of 70° unmodified in arenite layers. As the folds tightened, moving material out of the cores became more difficult (e.g. Chapple 1968, Hudleston 1973, Beutner 1978), and a phase of flattening took over to further tighten the fold and modify the mica-band cleavage/bedding angle. The strain ratio required at this stage, measured in the profile plane, is 1.4 to 1. Such a strain is compatible with shape factor measurements on quartz grains from the Mondurup fold which show a mica-film based cleavage in arenite requires only a very low strain to become a recognisable field fabric. The above fold history fits the observed geometry and strain extremely well, whereas each of the other modelled histories failed to duplicate the Mondurup example in some respect.

Some features of the final state are difficult to explain in terms of straightforward models. The complex fabric/bedding relations in the fold closures appear to need a change in the position of the hinge point during folding.

The closures certainly reflect a complex strain history with fanned S_{1G} and departures from S_{1G} occupying the S_{1B}/bedding acute angle.

Much of this paper is concerned with the Mondurup multilayer but there are several variations in sedimentary layer arrangements in the region examined. At Toll Peak wackes alternate with fairly continuous mudrock layers and this sequence probably underwent more strain in the layer-parallel shortening stage. Strains associated with S_{1G} are seen to be higher, but this state would make the elimination of some of the hypothesised fold histories more difficult. Despite the greater fabric development, the S_{1G}/S_{1B} angles on the fold common limbs are greater (27.5° is the mean of ten readings from Toll Peak) than the Mondurup fold. The continuous slate horizons at Toll Peak must favour the body rotation of the wacke layers in the fold amplification phase of development. The other extreme of the multilayers present are examples of lenticular, wedge-shaped arenite layers with virtually no mudrock. These probably behave in quite a different fashion from sequences with appreciable mudrock or reasonably planar layers.

Acknowledgements—The University of Western Australia Research Fund assisted with some field expenses. Discussions with geologists of the Geological Survey of Western Australia working in the same region have proved valuable.

REFERENCES

Alvarez, W., Engelder, T. & Geiser, P. A. 1978. Classification of solution cleavage in pelagic limestones. *Geology* **6**, 263-266.

Baillie, P. W. & Williams, P. R. 1975. Sedimentary and structural features of the Bell Shale correlate (Early Devonian), Strahan Quadrangle, Western Tasmania. *Pap. Proc. R. Soc. Tasm.* **109**, 1-15.

Beach, A. 1977. Vein arrays, hydraulic fractures and pressure-solution structures in a deformed flysch sequence, S.W. England. *Tectonophysics* **40**, 201-225.

Beutner, E. C. 1978. Slaty cleavage and related strain in Martinsburg Slate, Delaware Water Gap, New Jersey. *Am. J. Sci.* **278**, 1-23.

Borradaile, G. J. 1979. Strain study of the Caledonides in the Islay region, S.W. Scotland: implications for strain histories and deformation mechanisms in greenschists. *J. geol. Soc. Lond.* **136**, 77-88.

Boulter, C. A. 1976. Sedimentary fabrics and their relation to strain-analysis methods. *Geology* **4**, 141-146.

Cave, R. 1978. Report of field excursion, 6th March 1977. In: Conference Report: Deformation of soft sediments. (edited by Fitches R. & Maltman A. J.) *J. geol. Soc. Lond.* **135**, 251.

Chapple, W. M. 1968. A mathematical theory of finite-amplitude rock-folding. *Bull. geol. Soc. Am.*, **79**, 47-68.

Clarke, E. de C., Phillips, H. T. & Prider, R. T. 1954. The Precambrian geology of part of the south coast of Western Australia. *J. Proc. Roy. Soc. West. Australia* **38**, 1-64.

Elliott, D. 1970. Determination of finite strain and initial shape from deformed elliptical objects. *Bull. geol. Soc. Am.* **81**, 2221-2236.

Fyfe, W. S. 1976. Chemical aspects of rock deformation. In: A discussion on natural strain and geological structure, organised by J. G. Ramsay and D. S. Wood, *Phil. Trans. R. Soc. Lond.* **A 283**, 221-228.

Geiser, P. A. 1974. Cleavage in some sedimentary rocks of the Central Valley and Ridge Province, Maryland. *Bull. geol. Soc. Am.* **85**, 1399-1412.

Gray, D. R. 1978. Cleavages in deformed psammitic rocks from southeastern Australia: Their nature and origin. *Bull. geol. Soc. Am.* **89**, 577-590.

Harris, A. L., Bradbury, H. J. & McGonigal, M. H. 1976. The evolution and transport of the Tay Nappe. *Scott. J. Geol.* **12**, 103-113.

Hudleston, P. J. 1973. An analysis of 'single-layer' folds developed experimentally in viscous media. *Tectonophysics* **16**, 189-214.

Lisle, R. J. 1977. Folding and cleavage determined during sedimentation: Comment. *Sed. Geol.* **9**, 69-74.

Means, W. D. 1975. Natural and experimental microstructures in deformed micaceous sandstones. *Bull. geol. Soc. Am.* **86**, 1221-1229.

Nicholson, R. 1978. Folding and pressure solution in a laminated calcite–quartz vein from the Silurian slates of the Llangollen region of N. Wales. *Geol. Mag.* **115**, 47-54.

Nickelsen, R. P. 1973. Deformation structures in the Bloomsburg Formation. In: *Structure and Silurian and Devonian Stratigraphy of the Valley and Ridge Province in Central Pennsylvania,* (edited by Faill, R.T.). Pennsylvania Bur. Topographic and Geologic Survey, Dept. Environmental Resources, 119-129.

Plessman, W. 1964. Gesteinslösung, ein Hauptfaktor beim Schieferungsprozess. *Geol. Mitt.* **4**, 69-82.

Price, N. J. 1975. Fluids in the crust of the earth. *Sci. Prog.* **62**, 59-87.

Ramsay, J. G. 1967. *Folding and Fracturing of Rocks.* McGraw-Hill, New York.

Ramsay, J. G. & Graham, R. H. 1970. Strain variation in shear belts. *Can. J. Earth Sci.* **7**, 786-813.

Ross, J. V. & Barnes, W. C. 1975. Development of cleavages within diamictites of Southeastern British Columbia. *Can. J. Earth Sci.* **12**, 1291-1306.

Sofoulis, J. 1958. The geology of the Phillips River, Goldfield, W. A. *Bull. geol. Surv. West. Australia,* **110**.

Turek, A. & Stephenson, N.C.N. 1966. The radiometric age of the Albany Granite and the Stirling Range Beds, Southwest Australia. *J. geol. Soc. Aust.* **13**, 449-456.